

## CRUSTAL STRUCTURE OF OAXACA, MEXICO, FROM SEISMIC REFRACTION MEASUREMENTS

BY CARLOS M. VALDES, W. D. MOONEY, S. K. SINGH, R. P. MEYER, C. LOMNITZ, J. H. LUETGERT, C. E. HELSLEY, B. T. R. LEWIS, and M. MENA

### ABSTRACT

Seismic refraction and gravity data have been analyzed to obtain a model of the compressional-wave velocity structure of the ocean-to-continent transition in the State of Oaxaca in southwestern Mexico. Crustal thickness on the continent at the latitude 18°N is  $45 \pm 4$  km, based on reflected phases from the Moho discontinuity. The crust has been modeled with three layers, with velocities of 4.3 to 4.6, 5.0 to 5.7, and 6.85 to 7.0 km/sec, each with positive velocity gradient. The crust thins to 10 km at the coast near Pinotepa Nacional, where Precambrian metamorphic rocks are exposed 45 km from the mid-America trench. Offshore, the oceanic structure consists of an 8-km-thick crust with a normal crustal velocity structure (Spudich and Orcutt, 1980). The apparent dip of the subducting plate beneath western Mexico is 10°. On the oceanic side, strong reflections suggest a minimum depth of 35 km for the lithosphere-asthenosphere boundary. The asthenosphere has a seismic velocity of 7.6 km/sec, and a thin lid in which the velocity is 8.6 km/sec.

### INTRODUCTION

The Middle America trench off the southwestern coast of Mexico is the site of northeastward subduction of the Cocos plate under the North America plate. In this area of rapid convergence, large interplate earthquakes have recurrence intervals of approximately 35 yr (Singh *et al.*, 1981; McNally and Minster, 1981). Our understanding of the seismicity and tectonics of this region is critically dependent upon our understanding of the seismic velocity structure. Unfortunately, measurements of crustal velocity structure in Mexico are sparse. With the data set presented here, we seek to define the crustal velocity structure in southwest Mexico, thus providing a framework for further investigations of seismicity and tectonics.

Previous studies of the crust in Mexico include a 400-km-long unreversed seismic refraction profile extending from Durango to the southeast, in the Central Altiplano (Steinhart and Meyer, 1961). The interpretation of this profile resulted in an earth model consisting of three layers of constant velocity (4.95, 6.01, and 7.63 km/sec) with the location of the continental Moho at 43 km depth. Couch and Woodcock (1981), using offshore seismic, gravity, and magnetic measurements near Acapulco, suggested a 9-km-thick oceanic crust dipping 2° under the continental margin. Hales *et al.* (1970) report a seismic refraction profile extending from San Luis Potosi into the Gulf of Mexico. They obtained a 6.0 km/sec average velocity for the continental crust and a depth to the Moho of 35 km. Crustal structure based on the analysis of surface wave dispersion has been reported by Fix (1975). He analyzed data from earthquake sources in Chiapas (southwest Mexico) recorded in Arizona, thereby obtaining an average crustal and upper mantle structure along the entire 2000-km-long path. Fix's model consists of three layers with shear velocities of 3.13, 3.40, and 3.57 km/sec, and thicknesses of 4.0, 14.2, and 6.18 km, respectively. He also suggests a 4-km-thick high-velocity lid for the top of the mantle at a depth of 30 km. Lomnitz (1982) and Nava *et al.* (1985) have developed models based on

travel times of some well-recorded earthquakes that shed light on the ocean-to-continent transition zone in southwest Mexico close to our area of study. In addition, travel times from well-recorded subduction-related earthquakes in Petatlan, Guerrero, have been used to infer an "optimum" velocity structure by minimizing station residuals (e.g., Valdes *et al.*, 1982). None of these studies allow the construction of a velocity cross-section of the ocean-to-continent transition at the seismically active western margin of Mexico. In order to provide data on this transition zone, a cooperative seismic refraction investigation was undertaken in the state of Oaxaca in 1974 by the Universidad Nacional Autonoma de Mexico (UNAM), the University of Texas at Dallas (UTD), the University of Wisconsin-Madison (UWM), and the University of Washington-Seattle (UWS). This paper presents the results of this study.

#### EXPERIMENT SETTING

The seismic refraction profile runs approximately north-south, nearly perpendicular to the coast (Figure 1). Two shots (500 kg each) were detonated by UNAM in Lake Alchichica, 200 km east of Mexico City, and 22 shots (15 to 600 kg) were fired by UWS offshore along a straight line perpendicular to the coast (Figure 1).

Recording stations were established at about 15 km intervals from Lake Alchichica to the coast. The stations at the northern end of the profile were equipped with six smoked-paper recorders operated by UNAM. The middle part of the line was occupied by UTD AM tape recording seismographs. The data was digitized and played back in seismic record sections. The southern end of the line was occupied by UWM using five FM tape recording seismographs. These records were also digitized for display in record sections. Timing was provided by radio time signals and internal chronometers. All seismographs were equipped with 1 Hz seismometers.

The locations of stations and shots on land were determined from topographic maps at a scale of 1:100,000 and are accurate to within 1000 m or better. The sea shots were located by satellite navigation to within 500 m. A total of 13 seismographs successfully recorded the lake shots; failure to obtain useful records at the other stations was due to instrument malfunction and local noise. In particular, the smoked-paper recordings of the first arrivals from the lake shots were of poor quality and consequently did not provide information about local shallow structure. The complete series of sea shots was well recorded by six seismographs distributed along the 100 km profile line.

Sea shots and seismic stations have been corrected to place them at the ocean bottom and at sea level, respectively. The corrections and locations are shown in Table 1.

#### GEOLOGY AND TECTONICS

In the eastern Pacific Ocean, the Cocos plate forms along the East Pacific Rise, moves northeastward in relation to the North America Plate, and underthrusts southwest Mexico and Central America in the vicinity of the Middle America trench (Molnar and Sykes, 1969; Minster *et al.*, 1974). The North American and the Cocos plates (or other lithospheric plates such as Farallon and Guadalupe) have been converging intermittently along the Pacific Mexican coast for at least 100 m.y. (de Czlerna, 1960; King, 1969; Coney, 1972; Urrutia-Fucugauchi, 1984).

The Mexican Pacific margin from 94°W to 106°W exhibits intriguing features not characteristic of older arc systems. First, there are no belts of subduction complexes (at least of Mesozoic or younger age) parallel to the arc system, and

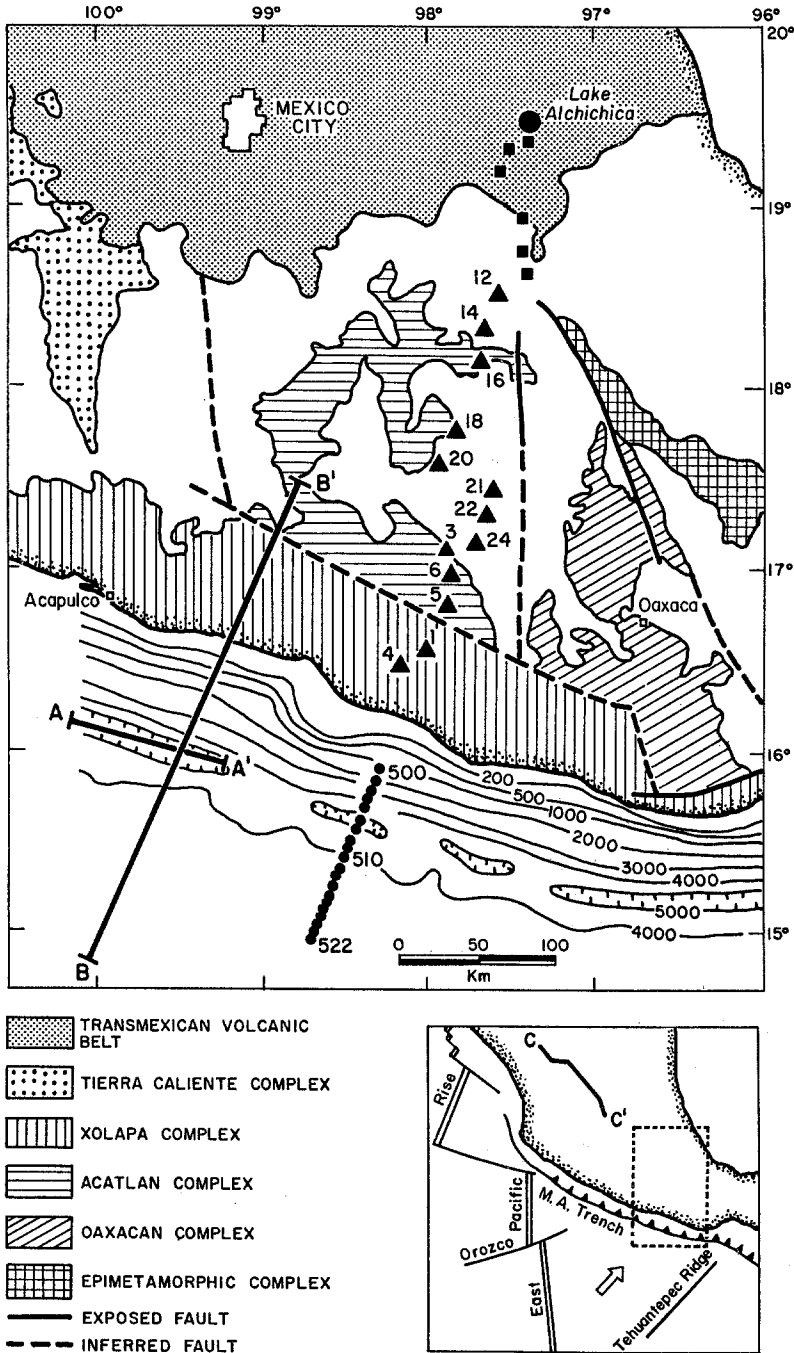


FIG. 1. Geologic map showing the distribution of crystalline terranes in southern Mexico (modified from Ortega-Gutierrez, 1981). Triangles represent sites occupied by AM and FM recording seismographs, and squares sites occupied by smoked-paper seismographs. Small circles indicate the offshore explosions, and the large circle the explosion at Lake Alchichica. Line A-A' shows the refraction profile study done by Shor and Fisher (1961). Line B-B' represents the gravity profile used by Couch and Woodcock (1981) to obtain crustal and subcrustal sections. The Steinhart and Meyer (1961) refraction line C-C' is shown in the index map.

TABLE 1  
STATION AND SHOT PARAMETERS

Station No.	Latitude (°N)	Longitude (°W)	Elevation (m)	Velocity* (km/sec)	Correction† (sec)
4	16.62	98.17	450	5.5	0.08
1	16.64	98.03	600	5.5	0.10
5	16.92	97.94	500	5.5	0.09
6	16.75	97.99	600	5.5	0.10
3	17.15	97.90	1500	5.5	0.29
24	17.19	97.93	2200	4.5	0.52
22	17.60	97.67	2100	4.5	0.50
21	17.44	97.64	2100	4.5	0.50
20	17.61	97.89	2200	4.5	0.52
18	17.79	97.83	1900	4.5	0.45
16	17.97	97.67	1700	4.5	0.40
14	18.14	97.69	1500	4.5	0.35
12	18.30	97.66	1900	4.5	0.45

Shot No.	Latitude (°N)	Longitude (°W)	Water depth (m)	Shot depth (m)	Weight (kg)	Correction‡ (sec)
1	16.032	98.299	790	200	900	0.42
2	15.991	98.316	1167	200	150	0.70
3	15.937	98.338	1397	213	150	0.85
4	15.884	98.362	1843	293	300	1.13
5	15.831	98.386	2791	210	150	1.89
6	15.779	98.409	3621	186	150	2.51
7	15.726	98.432	4546	263	300	3.13
8	15.675	98.454	5007	38	150	3.64
9	15.623	98.477	4700	71	150	3.38
10	15.572	98.499	4510	274	600	3.10
11	15.520	98.521	4214	45	150	3.04
12	15.495	98.532	4155	151	60	2.92
13	15.470	98.542	3689	246	150	2.51
14	15.419	98.564	3383	152	300	2.36
15	15.370	98.585	3795	132	150	2.68
16	15.345	98.596	3402	142	30	2.38
17	15.321	98.607	2941	142	150	2.04
18	15.272	98.628	3296	86	300	2.35
19	15.223	98.649	3517	162	150	2.45
20	15.199	98.659	3506	15	15	2.55
21	15.175	98.670	3321	156	150	2.32
22	15.127	98.689	3189	150	300	2.26

\* Velocity used to apply the correction.

† Elevation correction applied to each station to reduce the travel time to sea level, following a 5° slant path (the presumed path).

‡ Correction applied to each shot to reduce the travel time to the sea floor, following a 5° slant path (the presumed path).

second, the Middle America trench in this section is less than 75 km from the coast, much closer than the corresponding distance for other arc systems with long subduction histories (Karig and Sharman, 1975).

The profile crosses a highly varied geological setting (Figure 1). At its northern end, the profile traverses the late Cenozoic, trans-Mexican volcanic belt. Sixty kilometers south of Lake Alchichica, the profile enters a region dominated by Mesozoic sedimentary and metasedimentary rocks. Approximately 240 km south of the lake, the profile crosses the Acatlan Complex (early Paleozoic) composed of

metasediments, metavolcanics, metaophiolites, mylonitized granitoids, and a clastic unit (Ortega-Gutierrez, 1981). Between the shore and the Acatlan Complex, Ortega-Gutierrez (1981) identified the Xolapa Complex (Paleozoic-Mesozoic?) as being composed of migmatites, gneisses, and schists. Moore *et al.* (1982) obtained piston and drill cores within 35 km of the trench (inner slope) in an area 75 km NW of

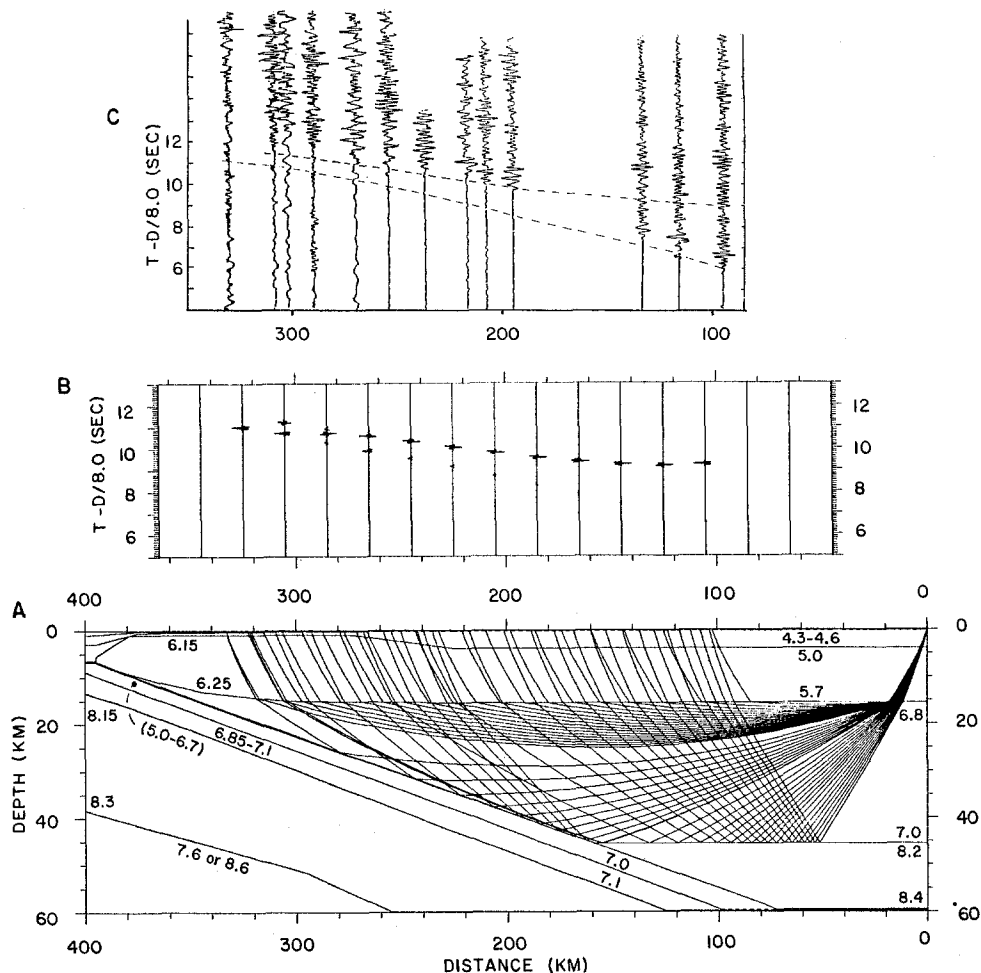


FIG. 2. (A) Structural model and ray tracing for the lake shot. The velocities are indicated in kilometers/second. (B) Synthetic seismograms for the model. A Ricker wavelet was used as a source function. (C) Record sections. The arrival times from the synthetic seismograms are marked with a dashed line. The weak arrivals correspond to turning rays in the lower crust. Large secondary arrivals correspond to reflections from the Moho and from top of the subducting oceanic lithosphere. The reflections from the Moho constrain the depth of that boundary. By changing the depth of the Moho and looking at the agreement between observed data and the synthetics, we estimate the depth to the Moho to be correct to within 4 km.

our profile. These cores confirmed the presence of schist from the Xolapa Complex at a depth of 320 m under the ocean floor.

#### SEISMIC ANALYSIS

To obtain a model for seismic *P*-wave velocity structure, we used a two-dimensional ray-tracing technique in which ray paths and *P*-wave travel times were calculated for successive modifications of an initial model until the computed travel

times agreed with the observed arrival times. The initial model of oceanic crust subducting under the continent was constrained by the results of studies by Steinhart and Meyer (1961), Couch and Woodcock (1981), and Ortega-Gutierrez (1981).

For the present study, we regarded a model as satisfactory when the difference between computed and observed travel times was less than 0.2 sec. Although we did not uniformly achieve this precision for all data points from each shot, we found that 90 per cent of the data were fitted to within  $\pm 0.2$  sec and 99 per cent to within  $\pm 0.3$  sec.

We used a ray-tracing algorithm developed by one of us (J.H.L.) as an implementation of a technique described by Červený *et al.* (1977) for calculating the propagation of rays through two-dimensionally inhomogeneous media. The model is divided into quadrilaterals by layer interfaces and vertical grid lines. The velocity within each quadrilateral is interpolated from specified values at the four corners.

In addition to travel times, waveform amplitudes were considered in the analysis of the profile. The amplitude data help constrain velocity gradients within layers

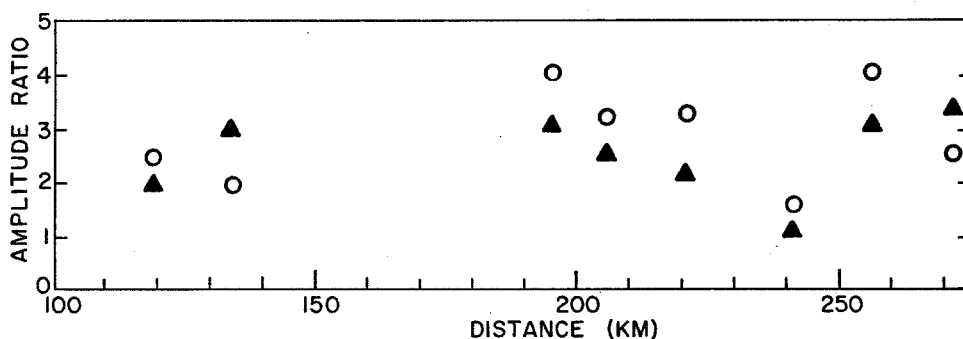


FIG. 3. Observed and calculated secondary over first arrival amplitude ratios as a function of distance for Lake Alchichica shot. Triangles are observed ratio amplitudes of the secondary over first arrival. Open circles represent ratio amplitudes of the secondary over first arrival from the synthetic seismograms. Amplitudes are peak to peak.

and can resolve uncertainties in phase correlations. For our data, true amplitude record sections were unavailable so that comparison of amplitudes on adjacent traces is not valid. However, the relative amplitudes of successive arrivals in each recorded trace may be compared with those in a synthetic seismogram trace. The synthetic seismograms were obtained using the modified asymptotic ray theory method developed by McMechan and Mooney (1980). In this algorithm, the waveform amplitude is determined by geometrical spreading and application of all the complex plane-wave transmission and reflection coefficients along the ray path. However, diffraction beyond caustics and in shadow zones is not considered, nor is anelastic attenuation.

The resolution and uniqueness of the two-dimensional models resulting from this forward, nonlinear modeling process are difficult to quantify, especially for a two-dimensional model based on a linear profile. The sensitivity of the interpretation procedure was investigated by perturbing the interfaces and gradients until the observed and calculated wave arrivals were no more than 0.2 sec apart. Thus, the perturbations allowed us to estimate a range of uncertainty for each major tectonic feature. These uncertainties are considered individually in the detailed discussion which follows.

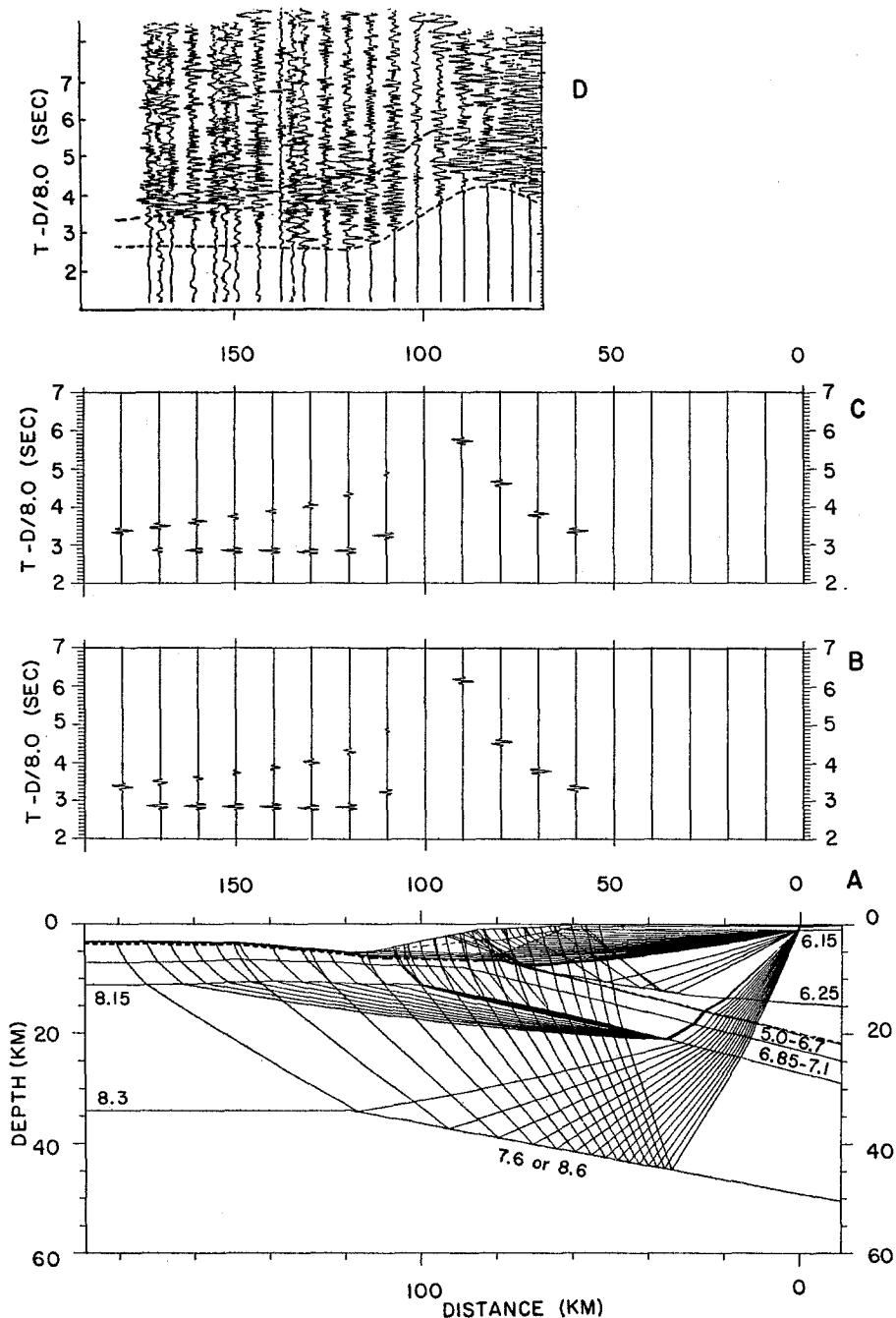


FIG. 4. Data recorded at station 1. (A) Ray trace diagram. The velocities (kilometers/second) at the top and bottom of each layer are indicated. (B) synthetic seismograms using a model with a 7.6 km/sec asthenosphere velocity. (C) synthetic seismograms using a model with a 8.6 km/sec asthenosphere velocity. (D) Observed data. The arrival times from the synthetic seismograms are marked with a dashed line. The first arrivals at the range of 70 to 85 km (D) are related to refracted rays on the top continental layer (A). In the range 85 to 165 km, the first arrivals correspond to rays refracted in the upper mantle. At a range of 140 to 165 km, large arrivals are observed at approximately 3.5 sec (D). We have modeled these arrivals as reflections from the dipping upper mantle horizon. This reflector dips 8° from 34 to 51 km depth, and we consider it as the lithosphere-asthenosphere boundary. No rays travel through the oceanic asthenosphere. However, the amplitude of reflected rays on the lithosphere-asthenosphere boundary is affected by the seismic velocity under this interface. (B) and (C) show synthetic seismograms using identical models except that the velocity in the asthenosphere is 7.6 or 8.6 km/sec, respectively. The latter model agrees better with the observed seismic data.

The recordings from the first lake shot are displayed in Figure 2. Recordings from the second lake shot are essentially identical to those from the first lake shot. This figure shows weak arrivals from rays turning in the lower crust, and strong secondary arrivals reflected at the Moho discontinuity, at a depth of about 45 km. Travel

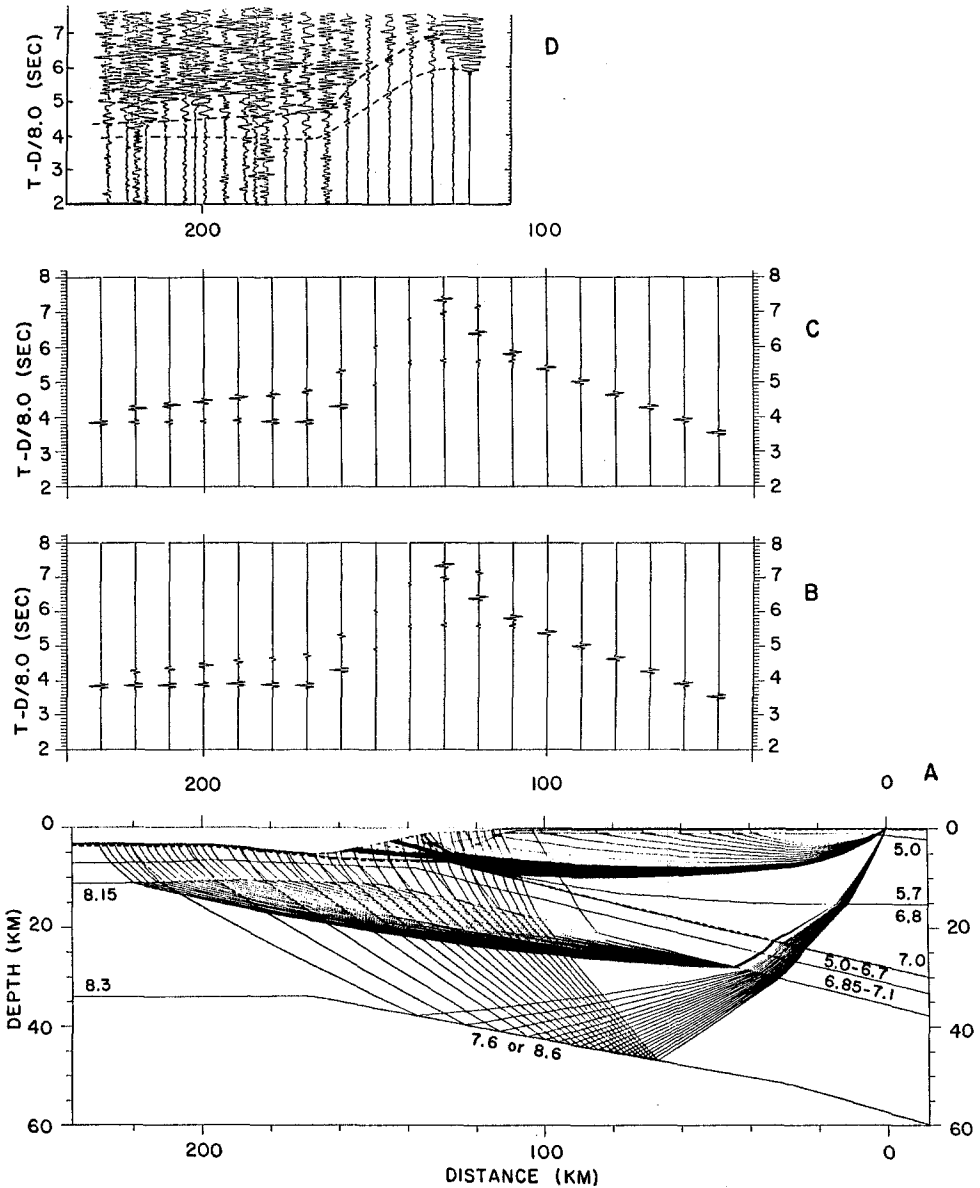


FIG. 5. Data recorded at station 3, Presentation as in Figure 4. The characteristics of the arrivals are similar to those in Figures 4 and 6.

times for these latter rays provide the only seismic information that we have to constrain the depth to the Moho. We estimate the depth of the Moho to be correct to within 4 km. Although ray paths from the lake shot (Figure 2) do not penetrate the upper mantle, the amplitudes of rays bouncing at the top of the upper mantle are sensitive to the velocities selected above and below the Moho. Figure 3 shows a

comparison of amplitude ratios of secondary over first arrivals between observed and synthetic seismograms. The preferred upper mantle velocity is between 8.2 and 8.4 km/sec, which is consistent with the upper mantle velocity determined by Steinhart and Meyer (1961).

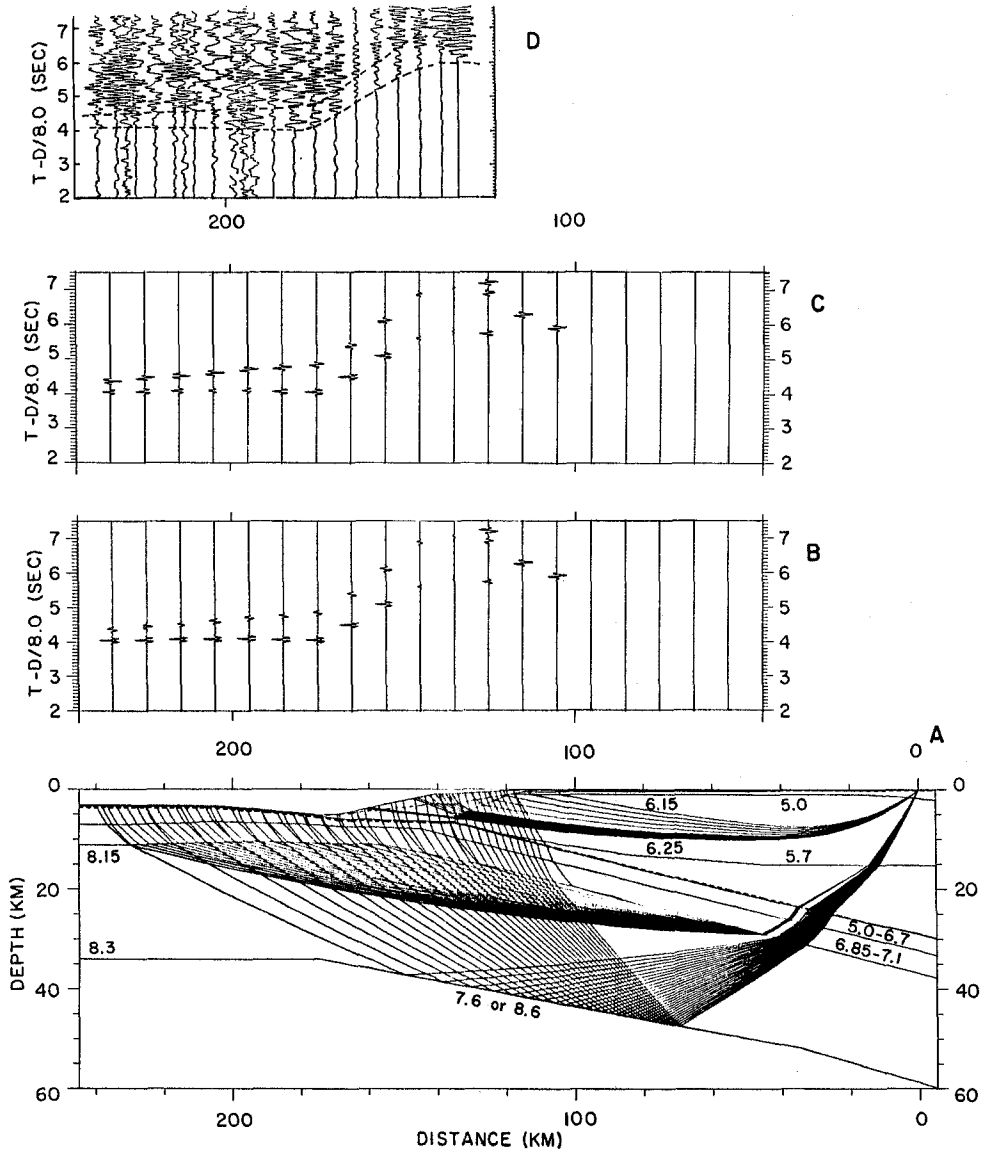


FIG. 6. Data recorded at station 6. Presentation as in Figure 4. The characteristics of the arrivals are similar to those in Figures 4 and 5.

The sea shots were recorded at stations 4, 1, 6, 3, 24, and 22, in order of increasing distance from the coast (Figure 1). Figures 4, 5, and 6 show data recorded at stations 1, 3, and 6, respectively, for the 22 sea shots. Figure 4D shows large first arrivals at the range of 70 to 85 km. We have modeled these arrivals as refracted rays on the second continental layer (Figure 4A). In the range of 85 to 165 km, the first arrivals are weak, except in the range of 100 to 130 km, where they become large. These

arrivals correspond to rays refracted on the upper mantle (Figure 4A). At a range of 140 to 165 km, large arrivals are observed at approximately 3.5 sec (Figure 4D). We have modeled these arrivals as reflections from the dipping upper mantle horizon. This reflector dips 8° from 34 to 51 km depth, and we consider it as the lithosphere-asthenosphere boundary. Rays that might travel through the oceanic asthenosphere are out of our observation range. However, the amplitude of reflected rays on the lithosphere-asthenosphere boundary is affected by the seismic velocity under this interface. Figure 4 (B and C) shows synthetic seismograms using identical models except that the velocity in the asthenosphere is 7.6 or 8.6 km/sec, respectively. The latter model agrees better with the observed seismic data.

However, the gravity anomaly from such a model does not match the observed gravity data. This discrepancy will be discussed later. Figures 5 and 6 are similar to Figure 4. Figure 7D shows the observed data from shot 510 recorded at seven stations. Reflections from the lithosphere-asthenosphere boundary and refractions from the lower lithosphere in Figure 7A agree with the large and weak arrivals of Figure 7D. By perturbing the dip of the lithosphere-asthenosphere boundary in the oceanic side of our model, we estimate it to be correct to within 2°.

#### GRAVITY DATA

Using the relationship between velocity and density presented by the compilation of Ludwig *et al.* (1970), the seismic model was converted to a two-dimensional density section (Figure 8). The major difference between the seismic velocity and density models is the replacement of blocks in which the velocity increases linearly with depth by blocks of constant density. Structurally, the only significant difference is the addition of an extra block of low density at a range of 140 km, which was necessary to match the broad positive peak in the gravity data. This extra block does not greatly affect the seismic results because only a few rays cross it. The travel time through this block is 0.4 sec.

Couch and Woodcock (1981) obtained a gravity profile 75 km NW from our study (Figure 1). They modeled the free air anomaly with a 50-km-thick lithosphere section, assuming no lateral variation in density below this depth. The upper part of Figure 8 shows our theoretical gravity profile, calculated following the method of Talwani *et al.* (1959). The agreement between our model and the observed anomaly [free air at sea (Couch and Woodcock, 1981); Bouguer on land], is very good. Our gravity model on the oceanic side differs from Couch and Woodcock's (1981) in that layers XI and XII (Figure 8) with densities 3.34 and 3.295 gm/cm<sup>3</sup> respectively, replace their 3.32 gm/cm<sup>3</sup> block.

#### INTERPRETATION

Three distinct blocks exist within the final model derived from seismic and gravity data: a continental block (units I thru IV); an accretionary block (units V thru VII); and an oceanic block (units VIII thru XII).

The velocity units within the continental block are related to geologic units identified by Ortega-Gutierrez (1981) and Lopez-Ramos (1983). In the oceanic block, the overall character of the interpreted velocity profiles closely resembles the seismic structure of oceanic crust elsewhere in the world (Spudich and Orcutt, 1980).

The continental velocity unit labeled I in Figure 8 is related to Jurassic and Cretaceous marine sediments and metasediments. The seismically determined depth agrees well with the estimate of 3 km given by Lopez-Ramos (1983). Unit II is

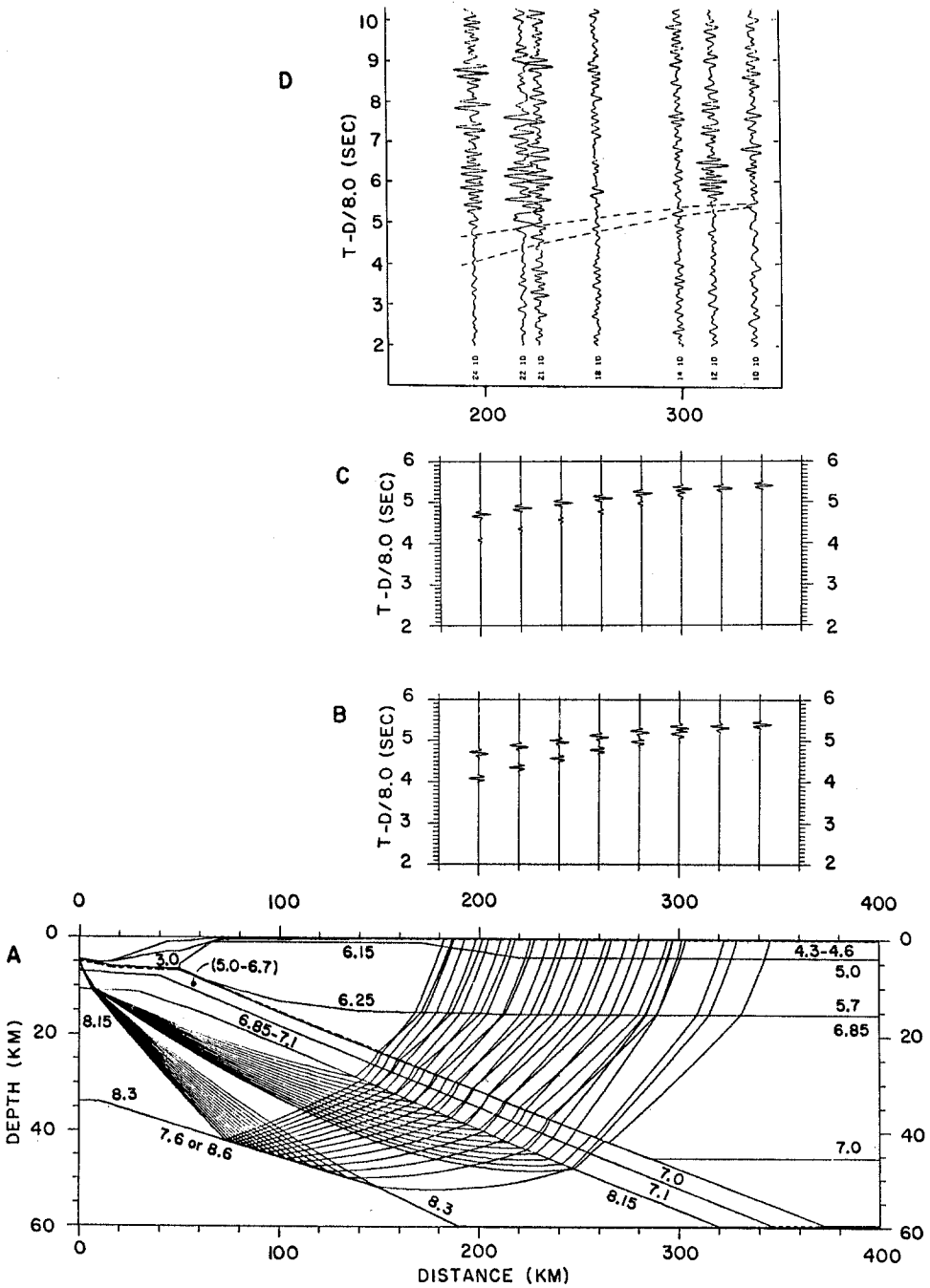


FIG. 7. Data recorded at seven stations from explosion 510. Presentation as in Figure 4. Strong reflections are from the upper dipping oceanic mantle; weaker arrivals are turning rays from the dipping upper oceanic mantle.

composed of two blocks. The block closer to the trench is associated with the Xolapa Complex, for which Ortega-Gutierrez (1981) suggests a minimum thickness of 15 km. The second block of unit II is related to the Acatlan Complex, for which Ortega-Gutierrez (1981) estimates a minimum thickness of 10 km. These depth

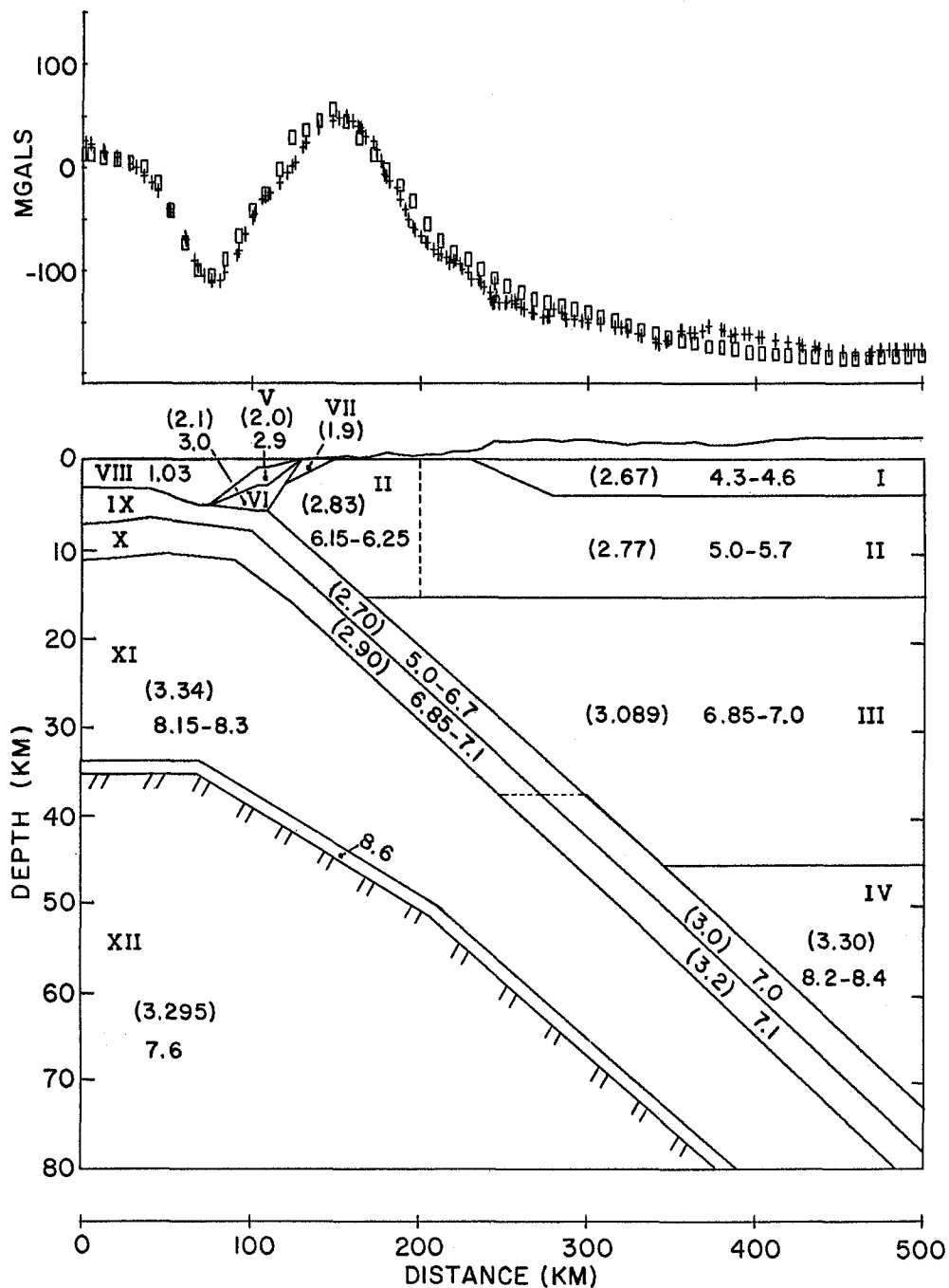


FIG. 8. Structural model for the area of study. The pair of numbers in each block corresponds to the velocity (kilometers/second) top and bottom of the layer. Dashed lines represent discontinuities in the velocity gradient. Block XII with a 7.6 km/sec seismic velocity represents the asthenosphere and has a 8.6 km/sec thin lid. The relation between seismic velocity and density of Ludwig *et al.* (1970) guided the selection of model densities (in parentheses, in gm/cm<sup>3</sup>) used to calculate the gravity anomaly, represented by squares. The crosses represent free air anomaly on the oceanic side (from Couch and Woodcock, 1981) and Bouguer anomaly on the continental side.

estimates are supported by the seismically determined depth of unit II in our model. The geological composition of the deep crust (unit III) is uncertain, but our determination of velocities greater than 6.8 km/sec is consistent with high-grade metamorphic rocks and mafic intrusive rocks. Our data indicate that the Moho is located at  $45 \pm 4$  km depth.

Units V, VI, and VII are interpreted as Tertiary and Quaternary sediments of the continental shelf and slope. Moore *et al.* (1982) identified this accretionary block as thick-bedded sand and mudstone, with slopes dominated by mud. Shipley *et al.* (1980) reports *P*-wave velocities of 2.2 to 3.5 km/sec for this accretionary zone.

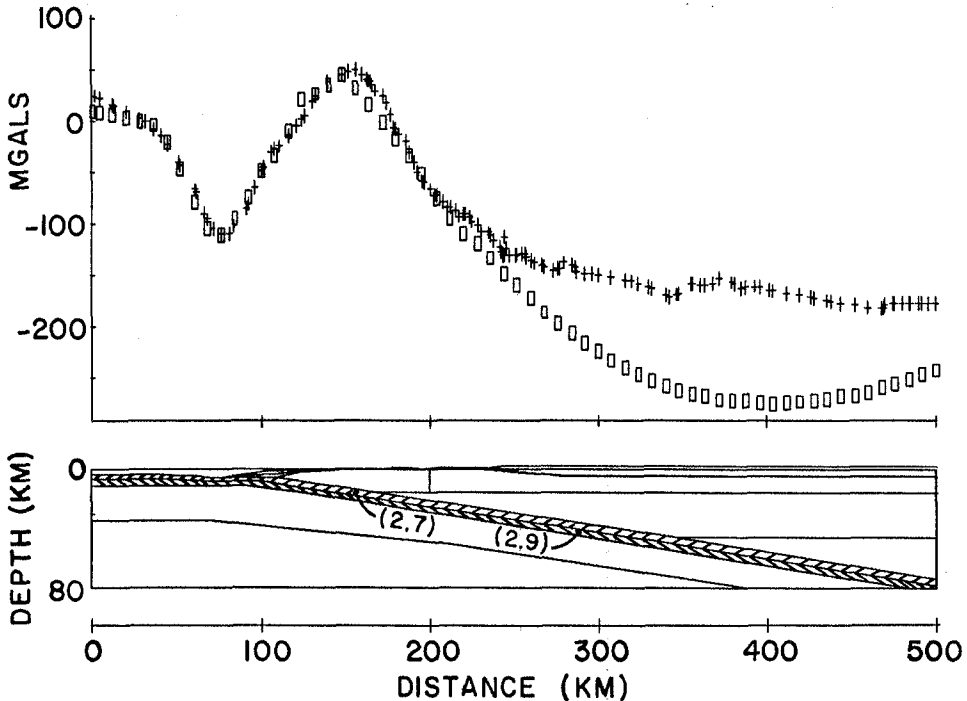


FIG. 9. Gravity model identical to that in Figure 8, except that the density in the dipping oceanic crust (blocks IX and X, Figure 8) is kept constant. This change shifts the calculated gravity anomaly (squares) 100 mgals from the observed gravity (crosses). The offset was corrected by increasing the density in the oceanic crust (blocks IX and X, Figure 8) below a depth of 35 km. A similar observation was found by Grow and Bowin (1975) in the Chile subduction zone. They explained it as a phase change from basalt to eclogite and from plagioclase peridotite to garnet peridotite.

Unit VIII is the water column. A sedimentary layer 180 m thick, with *P*-wave velocities of 1.7 to 1.9 km/sec, and composed of mud, mudstone, and pelagic clay, was drilled in the outer slope, 20 km from the trench in a site 75 km NW of our profile (Moore *et al.*, 1982). Such a thin layer, which would not cause substantial error in our calculations, has not been included in our model. Moore *et al.* (1982) found basalt immediately below the clay sediments; we identify unit IX with this oceanic basalt layer. Unit X is the oceanic lower crust and consists of metabasalts and gabbro. Units IX and X undergo abrupt transitions in velocity and velocity gradient, respectively, at a depth of 37 km in our model, which was required to obtain a better fit to the gravity data. Figure 9 shows the Bouguer anomaly obtained from a model that assumes a constant density for the dipping oceanic crust. Grow and Bowin (1975) interpreted shallow (30 km), high-density anomalies in the descending lithosphere beneath the Chile Trench, which they explained as a result

of phase change from basalt to eclogite and from plagioclase peridotite to garnet peridotite. From travel times of well recorded earthquakes, Lomnitz (1982) and Nava *et al.* (1984) found support for an inclined layer in the ocean-to-continent transition zone in southwest Mexico, close to the area of the present study. Nava *et al.* (1984) reported a thickness of 24 km for the layer with velocity of 7.5 km/sec dipping 13° from the trench toward the land. Units IX and X may correspond to the inclined layer proposed by Nava *et al.* (1984); however, the velocity, the thickness, and the dip differ. The boundary between units X and XI delineates the oceanic Moho. Unit XI is considered to represent the upper mantle, the lower

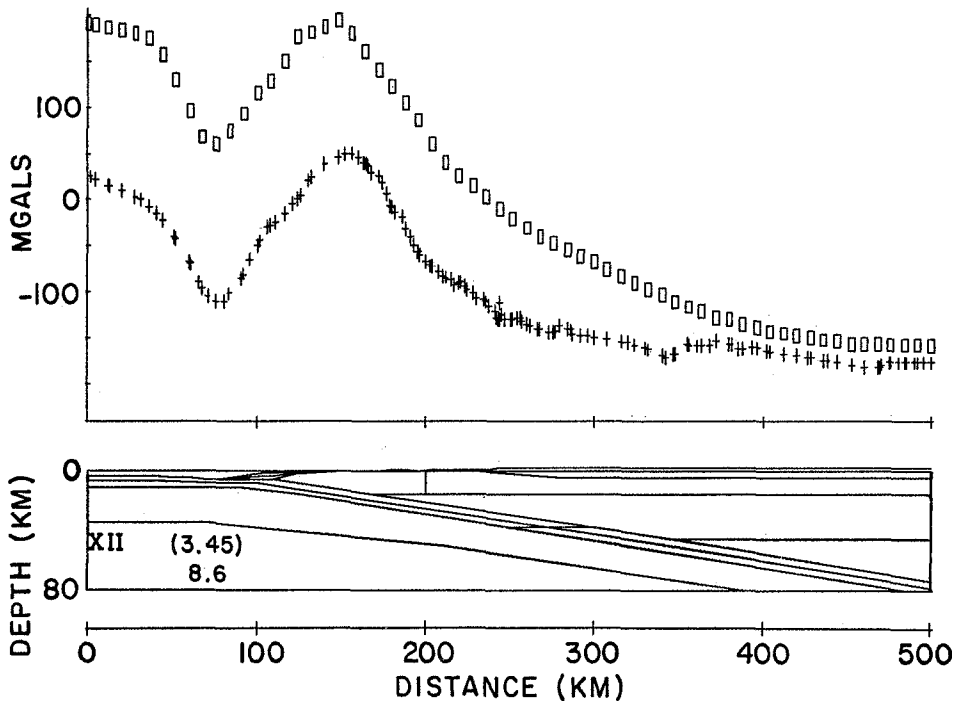


FIG. 10. Gravity model identical to that in Figure 8, except that block XII has a density of 3.45 gm/cm<sup>3</sup> instead of 3.295 gm/cm<sup>3</sup>. Such a model causes an offset of 180 mgals between the observed (crosses) and the calculated (squares) gravity anomaly.

boundary of which is constrained in part by a seismic reflector dipping 8° from 34 to 51 km depth, and dipping 10° below 51 km depth. The boundary between units XI and XII is interpreted as the boundary between the lithosphere and the asthenosphere.

We have tested possible upper asthenosphere velocities of 7.6 and 8.6 km/sec (block XII, Figure 8). The synthetic seismograms agree better with the observed seismic data if the velocity near the upper boundary of the asthenosphere is 8.6 km/sec instead of 7.6 km/sec [Figure 4 (B and C) to Figure 7 (B and C)]. Nonetheless, a material with a *P*-wave velocity of 8.6 km/sec corresponds to a minimum density of 3.45 gm/cm<sup>3</sup>, and such high density for all of block XII shifts the calculated anomaly 180 mgals from the observed values (Figure 10). On this basis, we suggest a third model with a low density, and presumably low velocity (7.6 km/sec), asthenosphere, and a thin high-velocity (8.6 km/sec) lid. Such a model satisfies both the seismic and the gravity data. A similar high-velocity zone (8.5 to 8.6 km/sec) in the subcrustal oceanic lithosphere has been found in the western

North Atlantic Ocean (LADLE, 1983). Spence *et al.* (1984, 1985) have also pointed out the difficulty in positively determining the seismic velocity (7.7 or 8.6 km/sec) for the asthenosphere at the Vancouver Island region, Canada.

The distance of about 600 km between the east Pacific Rise and the Middle America Trench at the area of our study, and the Cocos plate spreading rate of 108 mm/yr (Minster and Jordan, 1978) suggest an approximated age of 6 m.y. for the Cocos plate in this region. The young age of the lithosphere may explain its small thickness (34 km). A similar thickness is suggested by Spence *et al.* (1985) for the young (10 m.y.) Juan de Fuca plate in Vancouver Island.

A comparison of the final model (Figure 8) with Steinhart and Meyer's (1961) model shows similarity (within 2 km) in the depth of the continental Moho. However, the boundaries and velocities in the continental crust are different. They found four layers with velocities of 3.0, 4.95, 6.09, and 7.63 km/sec and thicknesses of 1, 3, 31, and 10 km, respectively. The vertical travel times of the two models agree within 0.1 sec. The thickness of the oceanic crustal layers determined by Couch and Woodcock (1981) is very similar to ours. However, their suggested 2° dip of the oceanic crust under the continental margin differs from the value we determine of 10°.

### CONCLUSIONS

We have obtained a seismic model for the ocean-to-continent transition in the southwest part of Mexico, consisting of a continental, an oceanic, and an accretionary block.

The continental block consists of three units (I to III, Figure 8) with the Moho located at 45 km depth ( $\pm 4$  km). The oceanic block (units IX to XII, Figure 8) has a crust 8 km thick, contained in an oceanic lithosphere 30 km thick. The 10° dip of the oceanic lithosphere under the continent is consistent with the fault plane dipping at an angle of 10° to 20° for large shallow thrust events near the area of study (Molnar and Sykes, 1969; Chael and Stewart, 1982; Singh *et al.* 1984; LeFevre and McNally, 1985). The oceanic lithosphere is underlain by a high velocity (8.6 km/sec), 2-km-thick lid. At a depth of 36 km, below the high-velocity lid, the oceanic asthenosphere is found. The proximity of the trench and the continental crust has been attributed to truncation of the continental margin (Moore *et al.*, 1982). Our model shows a continental crust very close (35 km) to the trench. However, it does not reveal the presence of sedimentary or metasedimentary layers on top of the subducting oceanic lithosphere, which might corroborate the hypothesis that the truncation is due to erosive subduction. The resolution of these features awaits higher quality marine seismic data.

### ACKNOWLEDGMENTS

We appreciate comments on this paper by Elizabeth Ambos, Luciana Astiz, Evelyn Roeloffs, and an anonymous reviewer. We also appreciate the helpful assistance of Lee Powell and William Unger during the field work. The assistance of the Comision Federal de Electricidad, Mexico, in arranging and providing for explosions in Lake Alchichica, is gratefully acknowledged. Federico Mooser collaborated in this phase of the investigation. This research was supported by National Science Foundation Grants GA40924, EAR8000048, and EAR8408451. Geophysical and Polar Research Center Contribution 442.

### REFERENCES

- Červený, V., I. A. Molotkov, and I. Psencik (1977). *Ray Method in Seismology*, Univerzita Karlova, Praha, Czechoslovakia, 214 pp.
- Chael, E. P. and G. S. Stewart (1982). Recent large earthquakes along the Middle America trench and their implications for the subduction process, *J. Geophys. Res.* **87**, 329-338.

- Coney, P. J. (1972). Cordilleran tectonics and North America plate motion. *Am. J. Sci.* **272**, 603–628.
- Couch, R. and S. Woodcock (1981). Gravity and structure of the continental margins of southwestern Mexico and northwestern Guatemala, *J. Geophys. Res.* **86**, 1829–1840.
- de Czerna, Z. (1960). Orogenesis in time and space in Mexico, *Geol. Rundschau.* **50**, 595–605.
- Fix, J. E. (1975). The crust and upper mantle of central Mexico, *Geophys. J. R. Astr. Soc.* **43**, 453–499.
- Grow, J. A. and C. O. Bowin (1975). Evidence for high density crust and mantle beneath the Chile Trench due to the decending lithosphere, *J. Geophys. Res.* **80**, 1449–1458.
- Hales, A. L., C. E. Helsley, and J. B. Nation (1970). *P* travel time for an oceanic path, *J. Geophys. Res.* **75**, 7362–7381.
- Karig, D. E. and G. F. Sharman (1975). Subduction and accretion in trenches, *Geol. Soc. Am. Bull.* **86**, 377–389.
- King, P. B. (1969). The tectonics of North America—A discussion to accompany the tectonic map of North America, scale 1:5,000,000, *U.S. Geol. Surv. Profess. Paper 628*, 95 pp.
- LADLE Study Group (1983). A lithospheric seismic refraction profile in the western North Atlantic Ocean, *Geophys. J. R. Astr. Soc.* **75**, 23–69.
- LeFevre, L. V. and K. C. McNally (1985). Stress distribution and subduction of aseismic ridges in the middle America subduction zone, *J. Geophys. Res.* **90**, 4495–4510.
- Lomnitz, C. (1982). Direct evidence of a subducted plate under southern Mexico, *Nature* **269**, 235–238.
- Lopez-Ramos, E. (1983). *Geologia de Mexico*, Vol. III, Mexico City, Mexico, 453 pp.
- Ludwig, W. J., J. E. Nafe, and C. L. Drake (1970). Seismic refraction, in *The Sea*, Vol. 4, Part 1, A. E. Maxwell, Editor, Interscience, New York, 53–84.
- McMechan, G. A. and W. D. Mooney (1980). Asymptotic ray theory and synthetic seismograms for laterally varying structures: theory and application to Imperial Valley, California, *Bull. Seism. Soc. Am.* **70**, 2021–2035.
- McNally, K. C. and J. B. Minster (1981). Nonuniform seismic slip rates along the Middle America Trench, *J. Geophys. Res.* **86**, 4949–4959.
- Minster, J. B. and T. H. Jordan (1978). Present-day plate motions, *J. Geophys. Res.* **83**, 5331–5334.
- Minster, J. B., T. H. Jordan, P. Molnar, and E. Haines (1974). Numerical modeling of instantaneous plate tectonics, *Geophys. J. R. Astr. Soc.* **36**, 541–576.
- Molnar, P. and L. R. Sykes (1969). Tectonics of the Caribbean and Middle America region from local mechanisms and seismicity, *Geol. Soc. Am. Bull.* **80**, 1639–1684.
- Moore, J. C., J. S. Watkins, T. H. Shipley, K. C. McMillen, S. B. Bachman, and N. Lundberg (1982). Geology and tectonic evolution of a juvenile accretionary terrane along a truncated convergent margin: Synthesis of results from the leg 66 of the Deep Sea Drilling Project, southern Mexico, *Geol. Soc. Am. Bull.* **93**, 847–861.
- Nava, F. A., V. R. Toledo, and C. Lomnitz (1985). Plate waves and the 1980 Huajuapán de León, Mexico earthquake, *Tectonophysics* **112**, 463–492.
- Ortega-Gutierrez, F. (1981). Metamorphic belts of southern Mexico and their tectonic significance, *Geofis. Internacional* **20**, 177–202.
- Shipley, T. H., K. J. McMillen, J. S. Watkins, J. C. Moore, J. H. Sandoval-Ochoa, and J. L. Worzel (1980). Continental margin and lower slope structures of the middle America trench Near Acapulco (Mexico), *Marine Geol.* **35**, 65–82.
- Shor, G. G., Jr. and R. L. Fisher (1961). Middle America trench: Seismic refraction studies, *Geol. Soc. Am. Bull.* **72**, 721–730.
- Singh, S. K., L. Astiz, and J. Havskov (1981). Seismic gaps and recurrence period of large earthquakes along the Mexican subduction zone: a reexamination, *Bull. Seism. Soc. Am.* **71**, 827–843.
- Spence, G. D., K. P. Whittall, and R. M. Clowes (1984). Practical synthetic seismograms for laterally varying media calculated by asymptotic ray theory, *Bull. Seism. Soc. Am.* **74**, 1209–1223.
- Spence, G. D., R. M. Clowes, and R. M. Ellis (1985). Seismic structure across the active subduction zone of western Canada, *J. Geophys. Res.* **90**, 6754–6772.
- Spudich, P. and J. Orcutt (1980). A new look at the seismic velocity structure of the oceanic crust, *Rev. Geophys. Space Phys.* **18**, 627–645.
- Steinhart, J. S. and R. P. Meyer (1961). Explosion studies of continental structure, Publication 622, Carnegie Institution of Washington, Washington, D.C., 409 pp.
- Talwani, M., J. L. Worzel, and M. Landisman (1959). Rapid gravity computations for two-dimensional bodies with application to the Mendocino submarine fracture zone, *J. Geophys. Res.* **64**, 49–59.
- Urrutia-Fucugauchi, J. (1984). On the tectonic evolution of Mexico: paleomagnetic constrains, In *Plate Reconstruction from Paleozoic Paleomagnetism*, Vol. 12, American Geophysical Union Geodynamic Series, Washington, D.C., 29–47.

- Valdes, C. M., R. P. Meyer, R. Zuniga, J. Havskov, and S. K. Singh (1982). Analysis of the Petatlan aftershocks: numbers, energy release and asperities, *J. Geophys. Res.* **87**, 8519–8527.
- Woodcock, S. (1975). Crustal structure of the Tehuantepec ridge and adjacent continental margins in southwestern Guatemala, *M.S. Thesis*, Oregon State University, Corvallis, Oregon, 52 pp.

DEPARTMENT OF GEOLOGY  
AND GEOPHYSICS  
UNIVERSITY OF WISCONSIN-MADISON  
1215 WEST DAYTON STREET  
MADISON, WISCONSIN 53706 (C.V., R.M.)

INSTITUTE OF GEOPHYSICS  
UNIVERSITY OF HAWAII  
2525 CORREA ROAD  
HONOLULU, HAWAII 96822 (C.H.)

U.S. GEOLOGICAL SURVEY  
345 MIDDLEFIELD ROAD  
MENLO PARK, CALIFORNIA 94025 (W.M., J.L.)

DEPARTMENT OF OCEANOGRAPHY  
UNIVERSITY OF WASHINGTON  
SEATTLE, WASHINGTON 98105 (B.L.)

INSTITUTO DE GEOFISICA  
UNAM  
CIUDAD UNIVERSITARIA  
MEXICO D.F., MEXICO (S.S., C.L., M.M.)

Manuscript received 2 July 1985